Journal of Physiology and Biochemistry (2019) 75:89–99
https://doi.org/10.1007/s13105-018-00660-6

ORIGINAL ARTICLE

LINGO-1 siRNA nanoparticles promote central remyelination in ethidium bromide-induced demyelination in rats

Alaa Eldin H. Youssef[1] · Abeer E. Dief[1] · Nesrine M. El Azhary[1] · Doaa A. Abdelmonsif[2,3] · Ola S. El-fetiany[1]

Received: 1 December 2017 / Accepted: 13 December 2018 / Published online: 13 February 2019
© University of Navarra 2019

Abstract

Multiple sclerosis is among the most common causes of neurological disabilities in young adults. Over the past decade, several therapeutic strategies have emerged as having potential neuroprotective and neuroregenerative properties. We investigated the effect of intranasal administration of LINGO-1–directed siRNA-loaded chitosan nanoparticles on demyelination and remyelination processes in a rat model of demyelination. Adult male Wistar rats were randomly assigned to one of 6 groups ($n = 10$ each) and subjected to intrapontine stereotaxic injection of ethidium bromide (EB) to induce demyelination. EB-treated rats were either left untreated or received intranasal LINGO-1–directed siRNA–chitosan nanoparticles from day 1 to day 7 (demyelination group) or from day 7 to day 21 (remyelination group) after EB injection. Chitosan nanoparticle (50 μl) was given alone after EB stereotaxic injection for both demyelination and remyelination groups. Two additional groups received 10 μl of saline by stereotaxic injection, followed by intranasal saline as controls for demyelination and remyelination groups ($n = 10$/group). Behavioural testing was conducted for all rats, as well as terminal biochemical assays and pathological examination of pontine tissues were done. After EB injection, rats had compromised motor performance and coordination. Pathological evidence of demyelination was observed in pontine tissue and higher levels of caspase-3 activity were detected compared to control rats. With LINGO-1–directed siRNA–chitosan nanoparticle treatment, animals performed better than controls. Remyelination-treated group showed better motor performance than demyelination group. LINGO-1 downregulation was associated with signs of repair in histopathological sections, higher expression of pontine myelin basic protein (MBP) mRNA and protein and lower levels of caspase-3 activity indicating neuroprotection and remyelination enhancement.

Keywords Demyelination · Remyelination · LINGO-1 · siRNA–chitosan nanoparticles · Myelin basic protein

Abbreviations

EB	Ethidium bromide
MBP	Myelin basic protein
OPCs	Oligodendrocyte precursor cells
SiRNA	Small interfering RNA

Electronic supplementary material The online version of this article (https://doi.org/10.1007/s13105-018-00660-6) contains supplementary material, which is available to authorized users.

✉ Abeer E. Dief
abeer.dief@alexmed.edu.eg

[1] Department of Medical Physiology, Faculty of Medicine, University of Alexandria, Alexandria, Egypt

[2] Department of Medical Biochemistry, Faculty of Medicine, University of Alexandria, Alexandria, Egypt

[3] Molecular Biology and Nanomedicine Labs, Centre of Excellence for Regenerative Medicine Research & Applications, University of Alexandria, Alexandria, Egypt

Introduction

Demyelinating diseases are a group of pathological conditions characterised by loss of the myelin sheath with demyelinating plaques surrounded by areas of inflammation and neurodegeneration. Multiple sclerosis is considered as the commonest of demyelinating disorder. The prevalence of multiple sclerosis differs greatly geographically, from below 5/100,000 in many areas of Africa, South America and Asia, to over 100/100,000 in Scotland and parts of Scandinavia and Canada [17].

Currently, there are no disease-modifying drugs that can efficiently slow, stop or reverse neurodegeneration in demyelinating diseases. However, in MS, neuroprotection may be conferred by another strategy namely myelin repair or

"remyelination" [26]. Remyelination is normally mediated by oligodendrocyte precursor cells (OPCs) in the brain parenchyma and in progenitor zones in the mature adult CNS. Deficient remyelination can occur in patients with MS either due to failure of OPC differentiation or recruitment to the lesion site. Therefore, therapeutic manipulations that improve recruitment and/or differentiation of OPCs may be beneficial for remyelination [7].

The remyelination process is actively suppressed by certain signalling pathways and mediators, including LINGO-1 protein, which is selectively expressed in neurons and OPCs. Suppression of LINGO-1 by different strategies as LINGO-1 gene knockout or infusion of LINGO-1 antagonists was associated with enhancement of remyelination in different animal models of CNS demyelination, and showed promising results in the treatment of demyelinating and neurodegenerative diseases [15]. Moreover, administration of anti-LINGO-1 antibodies was effective in enhancing remyelination. However, studies using anti-LINGO-1 (BIIB033), a monoclonal antibody specific to the LINGO-1 protein designed to promote remyelination, show that the antibody has low CNS penetration and thus needs to be administered in high doses to be effective [30, 35].

RNA interference is a new strategy to block LINGO-1 expression in the target lesions with low doses and less systemic side effects. Efficient delivery of small interfering RNAs (siRNAs) remains a challenge and much research has been aimed at developing ideal gene delivery carriers. In the last few years, chitosan nanoparticles have become one of the most studied polymers in non-viral siRNA delivery, due to their polycationic nature and biocompatibility [13]. The intranasal route of administration is a non-invasive method to bypass the BBB and directly deliver drugs to the CNS [13]. Chitosan has been widely used through intranasal route to deliver drugs to the brain as nerve growth factors and insulin [13]. In the present work, we investigated whether nasal administration of LINGO-1–directed siRNA-loaded chitosan nanoparticles in rats could inhibit pontine LINGO-1 expression and enhance remyelination in a model of demyelination induced by ethidium bromide (EB).

Material and methods

Experimental animals

All applicable international, national, and/or institutional guidelines for the use of animals were followed and animals were kept in accordance with the guidelines issued by the Ethics Committee of Alexandria faculty of Medicine. Adult male Wistar rats aged 10 weeks and weighing 250–300 g were kept under standard laboratory conditions, maintained on a 12-h light–dark cycle, with free access to standard lab chow and water. Rats were divided randomly into 2 main groups, EB groups and control groups. Treatment started 2 h after EB injection in the demyelination-treated group ($n = 20$) with either intranasal administration of 50 μl of nanoparticle solution (containing 2 μg siRNA/ml) or 50 μl of nanoparticle solution only via intranasal route in awake rats daily at 11 am and continued till day 7 [23].

Remyelination-treated group ($n = 20$) received the same dose of nanoparticle solution only or nanoparticle solution containing 2 μg siRNA/ml starting from day 7 after EB therapy (i.e. when demyelination had been confirmed) up to day 21 to detect the potential effect of siRNA nanoparticles on enhancement of remyelination.

Two positive control groups received a single stereotaxic injection of 10 μl of 0.1% EB, and 50 μl intranasal saline daily from day 1 to day 7 ($n = 10$) or from day 7 to day 21 ($n = 10$). Two additional groups received 10 μl of saline by stereotaxic injection, followed by intranasal saline as described above acting as negative controls for demyelination and remyelination groups ($n = 10$/group).

Stereotaxic surgery

Rats were anaesthetized by a mixture of intraperitoneally injected ketamine and xylazine (80–100 mg ketamine and 10 mg xylazine per kilogramme body weight. Focal demyelination in the rat pons was induced by a single stereotaxic injection of 10 μl of 0.1% EB (Promega Inc., Madison, WI) dissolved in isotonic (0.9% NaCl) saline solution immediately before use [4]. The following coordinates were used for targeting the white matter tracts which are located ventrally in pons: 9 mm posterior, 9 mm ventral, and 1.4 mm lateral to the bregma according to the Atlas of Paxinos and Watson.

Preparation of chitosan–siRNA nanoparticles

LINGO-1 siRNA was purchased from Abcam (Cambridge, MA). The ionic gelation method was used to formulate the nanoparticles. The negatively charged components, i.e. siRNA (50 μm) and sodium tripolyphosphate (TPP) (Sigma Aldrich Inc., St. Louis, MO) (1 mg/mL), were added to the positively charged components, i.e. chitosan (1 mg/mL in sodium acetate buffer 0.2 M, pH 5.5), and then vortexed for 30 s. The mix was left for 1 h and centrifuged for 30 min at 17,860×*g* [32]. In order to avoid RNAse contamination, strict RNAse-free conditions were followed, and all solutions were prepared in RNAse-free water and filtered through 0.22-μm filters. Furthermore, chitosan and all solutions were treated with the RNAsecure reagent (Ambion, Belgium). Furthermore, the loading efficiency of the siRNA-LINGO-1 in the siRNA-loaded chitosan nanoparticles was analysed using NanoDrop 1000 Spectrophotometer (Thermo Scientific, USA) at 260 nm in the supernatant solution

obtained after the synthesis of siRNA-loaded chitosan nanoparticles. Supernatants recovered from blank nanoparticles (without siRNA) were used as a blank. The siRNA loading efficiency was measured as the percentage of entrapped or adsorbed siRNA to the total amount of siRNA added where siRNA loading efficiency was found to be around 20% [21].

Behavioural testing

Rats were evaluated on day 7 after EB injection in the demyelination groups, as well as on days 7 and 21 in the remyelination groups, for clinical signs of demyelination and to detect the effect of nanoparticle and siRNA nanoparticles on the treated groups. All behavioural tests were conducted by researchers blind to group identity and performed between 9 and 12 am.

Rats that showed signs of altered cerebellar functions such as head or neck tremors, or vestibular alterations such as head tilt and walking in circles, were excluded from the experiment.

1. *Beam balance test*: Beam balance is a sensitive test for fine motor coordination and vestibulo-motor function. Each rat was placed on an elevated horizontal beam (25 mm in diameter, 60 cm in length), with illumination at the start side [19]. Each rat was trained to walk on the beam and the following six-point scoring system was used to measure beam-balance performance. 0 = Balances with steady posture, 1 = grasps side of the beam, 2 = hugs the beam with one limb falls from the beam, 3 = hugs the beam and two limbs fall from the beam or spins on the beam (> 60 s), 4 = attempts to balance on the beam but falls off (> 40 s), 5 = attempts to balance on the beam but falls off (> 20 s), and 6 = falls off with no attempt to balance or hang onto the beam (< 20 s).
2. *Foot fault test*: This test evaluates strength of the paws. Briefly, rats were placed on an elevated grid floor (40 × 40 cm with grid openings 3 cm^2) with their paws on the wire frame while moving along the grid. The foot fault was recorded when the paw fell or slipped through the wire, during each weight-bearing step. The number of foot faults was recorded from a total number of 50 steps for each limb [21].
3. *Rotarod test*: It assesses motor function and gross coordination. It consists of a rotating drum that can be accelerated from 4 to 40 rpm over the course of 5 min. All rats were trained on the rotarod for five trials/day for 3 days then each rat was placed individually on the drum and the latency of falling down from the drum was recorded [19].
4. *Inverted screen test*: This test measures fore-paw grip strength. An invertible screen of a 43 cm^2 of wire mesh consisting of 12 mm squares of 1 mm diameter was used. The screen was held steadily 40–50 cm above a padded surface. Rats were placed in the centre of the wire mesh screen. Then, the screen was rotated to an inverted position over 2 s. Using a stop watch, the time taken by the rat to fall off the mesh was recorded and scored as follows: 1 = falling between 1 and 10 s, 2 = falling between 11 and 25 s, 3 = falling between 26 and 60 s, 4 = falling after 60 s [1].

Termination and brain tissue sample preparation

Rats were subjected to terminal ether anaesthesia at days 7 or 21 in the demyelination and remyelination groups respectively. Pontine tissue samples were collected, rinsed with ice cold phosphate-buffered saline (PBS) and weighed. Samples were stored at − 80 °C for assessment of the expression level of LINGO-1 and myelin basic protein (MBP) mRNAs and protein, and caspase-3 activity.

LINGO-1 and MBP mRNAs expression by quantitative RT-PCR

Total RNA was extracted from pontine tissue using RNeasy Mini Kit (Qiagen, Hilden, Germany) under strictly sterile and RNAse-free conditions. RNA quality was then spectrophotometrically determined at 260/280 nm. In order to synthesise complementary deoxyribonucleic acid (cDNA), reverse transcription was performed in 25 μl reaction volume with 100 ng of total RNA, random hexamer primer and reverse transcriptase (RT) Superscript II (Invitrogen, USA). Subsequently, qPCR was performed in a 25 μl reaction volume containing 1X SYBR® Green PCR Master Mix (Applied Biosystems, USA) using One Step Real-Time PCR system (Applied Biosystems, USA). The specific primer pair for LINGO-1 was the sense primer AGAGACATGCGATTGGTGA and the antisense primer AGAGATGTAGACGAGGTCATT (GenBank AAH11057). As for MBP, specific primer pair was the sense primer GGCAAGGACTCACACACAAGAA and the antisense primer CTTGGGTCCTCTGCGACTTC (GenBank AC 000086). The amplification consisted of one cycle at 95 °C for 30 s followed by 40 cycles of denaturation at 95 °C for 5 s, an annealing step for 10 s, and an extension step at 72 °C for 20 s [9, 24]. The annealing temperature was modified to be 60 °C and 64 °C for LINGO-1 and MBP, respectively. Melting curve analysis of products was done after amplification to confirm the identity of the PCR products. A negative control without cDNA was run with every PCR to evaluate the specificity of the reaction. Data analysis was performed using StepOne™ Software v2.3 where the level of expression of LINGO-1 and MBP was determined by the comparative CT method for gene expression relative to the housekeeping gene glyceraldehyde 3 phosphate dehydrogenase (GAPDH).

LINGO-1 and MBP protein expression by Western blot

For determination of LINGO-1 and MBP protein expression, a part of the pontine tissue was homogenised in ice cold radioimmunoprecipitation (RIPA) lysis buffer (1× Tris-buffered saline, 1% Nonidet P 40, 0.5% sodium deoxycholate, 0.1% sodium dodecyl sulfate, 0.004% sodium azide) containing phenylmethanesulfonyl fluoride solution (PMSF), sodium orthovanadate (Na3VO4) and both protease inhibitor cocktail (Sigma-Aldrich, St. Louis, MO, USA). Homogenates were centrifuged at 15,000 rpm for 15 min at 4 °C. Total protein concentration was assessed by the bicinchoninic acid (BCA) protein quantitation kit (Sigma-Aldrich, St. Louis, MO, USA) [37]. Next, 30 μg of tissue protein was subjected to sodium dodecyl sulfate-polyacrylamide gel electrophoresis (SDS-PAGE). Blotting of the separated proteins to nitrocellulose membrane (Bio-Rad, Mississauga, ON, Canada) was next done using a Trans-Blot apparatus (Bio-Rad). The membranes were stained in order to confirm the uniform transfer of samples. Then, the membranes were blocked using bovine serum albumin (BSA, 5%) at room temperature for 1 h and were incubated with the specific primary antibodies for 2 h at room temperature. Afterwards, the membranes were washed in 1X Tris-buffered saline (TBST; pH 7.4) and incubated with the HRP-conjugated secondary antibody for 1 h. Lastly, the membranes were washed in TBST and then PBS, and protein bands were visualised using 3,3′,5,5′-tetramethylbenzidine (TMB) stain. The dilutions of the primary antibodies were as follows: anti-LINGO-1 antibody (ab2363, 1:1000), anti-MBP antibody (ab40390, 1:1000) or β actin (A5316, 1: 4000). Quantity One software (Bio-Rad Laboratories, USA) was used for quantification of protein bands where protein expression was normalised to the β-actin protein and the control group.

Caspase-3 activity

A part of the pontine tissue was homogenised in caspase-3 reaction buffer. Pontine caspase-3 enzymatic activity was measured by colorimetric reaction provided by R&D Systems Inc., Germany. Results were normalised to total tissue protein and were expressed as a ratio to the baseline (control) levels [11].

Histopathological examination

Pontine tissues were collected after decapitation, fixed overnight at 4 °C with 4% paraformaldehyde, then specimens were placed in 10% neutral formalin solution, processed and embedded in paraffin for histological examination. Coronal sections of pons (5 μm thick) were cut with microtome, and stained with both Luxol fast blue (LFB) and haematoxylins & eosin (H&E) then analysed using a light microscope.

Statistical analysis

Data were analysed using PASW Statistics for Windows (21.0; SPSS Inc., Chicago, IL, USA) and graphs were prepared using GraphPad Prism (version 6.0f for windows). Data were expressed as mean ± SD. Tests of significance were two tailed and $p < 0.05$ was considered statistically significant. Multiple variables were evaluated by one-way ANOVA test, followed by a post hoc Tukey test for pairwise comparisons. Results for beam balance and foot fault tests were expressed as median values and analysed by Kruskal-Wallis test followed by Mann-Whitney *U* test for comparison.

Results

In the current study, there were no reported deaths during the stereotaxic or other experiment procedures. Meanwhile, five rats showed signs of cerebellar and vestibular dysfunction so they were replaced by other rats.

Effect of different treatment regimens with LINGO-1–directed siRNA-loaded nanoparticles on motor performance

EB injection led to significant impairment of motor power as evidenced by increased number of failure in the beam balance test with decreased time spent by rats on the beam ($p < 0.001$). Foot slippages recorded from foot fault test were markedly increased after EB injection compared to controls (median of 3.5 in demyelination group and 2 remyelination group versus 0 in controls). When tested on the rotarod, EB rats featured a decrease in the mean latency to fall in both the demyelination (56.6% compared to control) and remyelination (47.8% compared to controls). Moreover, duration of grasp strength as measured by inverted screen test was significantly decreased in the EB groups ($p < 0.001$). Notably, that rats in the remyelination group whether untreated or received chitosan nanoparticles only (after 21 days of EB injection) showed better motor performance (foot fault test) than untreated demyelination group, i.e. after 7 days of EB injection ($p < 0.05$).

Both early and delayed treatment with LINGO-1–directed siRNA-loaded nanoparticles significantly improved balance and coordination in the beam balance test, with rats achieving scores near to controls. Paw strength was significantly improved as evidenced by marked reduction in the number of foot slippage after treatment compared to untreated EB groups. Latency to fall off rotarod was markedly increased after LINGO-1–directed siRNA-loaded nanoparticles treatment compared to EB group. However, the motor performance was still significantly less than controls. In the foot fault test, delayed treatment with LINGO-1–directed siRNA-loaded nanoparticles (day 7–21) was more effective in

reversing the EB abnormalities compared to early treatment (day 1–7; Fig. 1a–d).

Treatment with chitosan nanoparticle alone did not exert the same degree of improvement in the motor deficits when compared to LINGO-1 treated groups.

LINGO-1–directed siRNA-loaded nanoparticles enhanced MBP expression and decreased apoptosis

The MBP mRNA and protein signal in pontine tissue measured on day 7 after EB injection was not different from the control group. However, on day 21, MBP mRNA and protein were induced 4-fold in the untreated EB group compared to controls. siRNA-loaded nanoparticle treatment was associated with significant increase in MBP mRNA and protein expression when started early from day 1–7 and a more prominent increase when started late (7–21 days) relative to controls ($p < 0.001$; Fig. 2a, b, f). It is worth mentioning that the administration of the unloaded chitosan nanoparticles was accompanied by increased MBP mRNA and protein expression when started early from day 1–7 and late (7–21 days) relative to ethidium bromide–injected group. Yet, coupling LINGO-1 siRNA with chitosan nanoparticles resulted in a remarkable increase in MBP expression. This denotes the possible implication of chitosan nanoparticles by itself in improving the regenerative process in MS.

Apoptosis, evidenced by enhanced caspase-3 activity, was increased by EB injection at day 7 and day 21 (Fig. 2e). LINGO-1–directed siRNA-loaded nanoparticle treatment protected against neural apoptosis, as evidenced by decreased caspase-3 activity in both the early and delayed treated groups. The different treatment regimens were comparable in their effect on caspase-3 activity levels. Interestingly, LINGO-1 siRNA-loaded nanoparticle treatment was able to normalise caspase-3 activity in the delayed treatment group as evidenced by the insignificant difference from the control group. A related point to consider was decreased neural apoptosis after both early and delayed chitosan nanoparticle administration further highlighting its potential effect in alleviating the pathology of MS and enhancing the effect of the coupled siRNA.

LINGO-1–directed siRNA-loaded nanoparticles suppressed pontine LINGO-1 expression

EB injection did not alter LINGO-1 mRNA or protein expression in pontine tissue in both untreated EB-injected groups. On the other hand, both early and delayed treatment with LINGO-1–directed siRNA-loaded nanoparticles markedly decreased LINGO-1 mRNA and protein expression in pontine tissue ($p < 0.001$ each versus respective untreated EB groups), with no significant difference between early and delayed treatment (Fig. 2c, d, f). In the meantime, chitosan nanoparticles early or delayed treatment decreased LINGO-1 protein, but

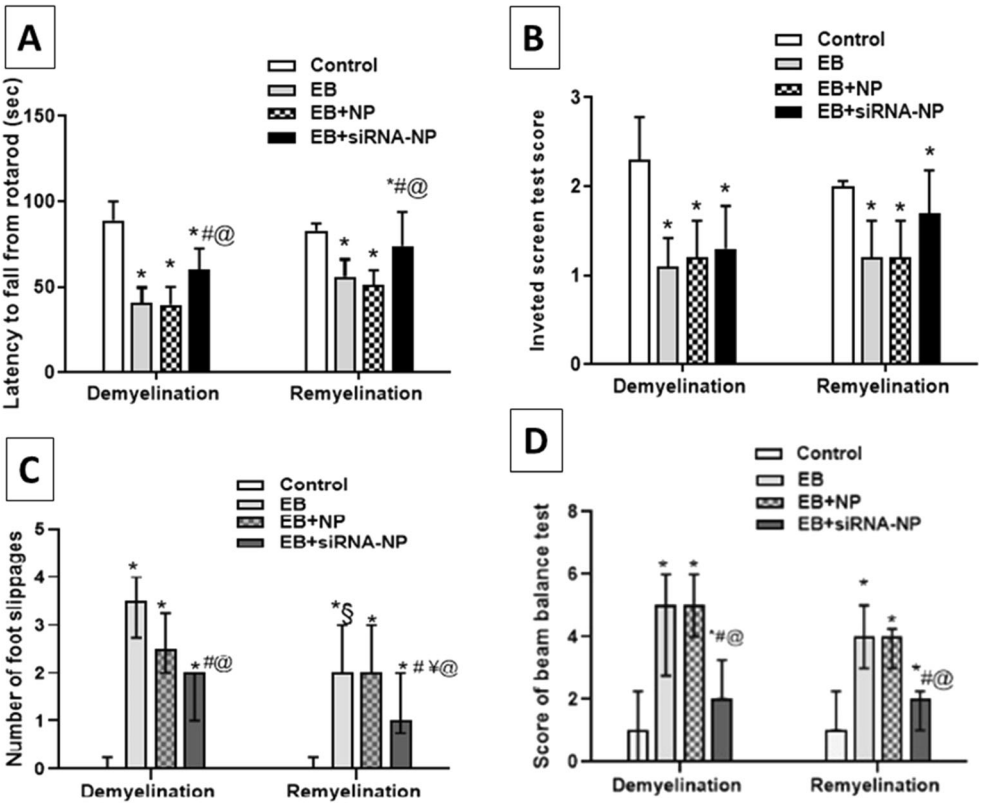

Fig. 1 Effect of ethidium bromide (EB) injection and treatment with LINGO-1–directed siRNA-loaded nanoparticles or chitosan nanoparticles on latency to fall from rotarod (**a**), inverted screen score (**b**), number of foot slippage (**c**), and beam balance test (**d**). Values are mean ± SD for **a**, **b** and median (25th, 75th percentiles) for **c**, **d** from $n = 10$/group. Significant post hoc or Mann-Whitney *U* test is indicated by asterisks $*p < 0.05$ versus corresponding control group, $\#p < 0.05$ versus corresponding ethidium bromide group, $@p < 0.05$ versus corresponding EB + NP groups, $§p < 0.05$ between ethidium bromide groups, $¥p < 0.05$ between the EB + siRNA-NP groups

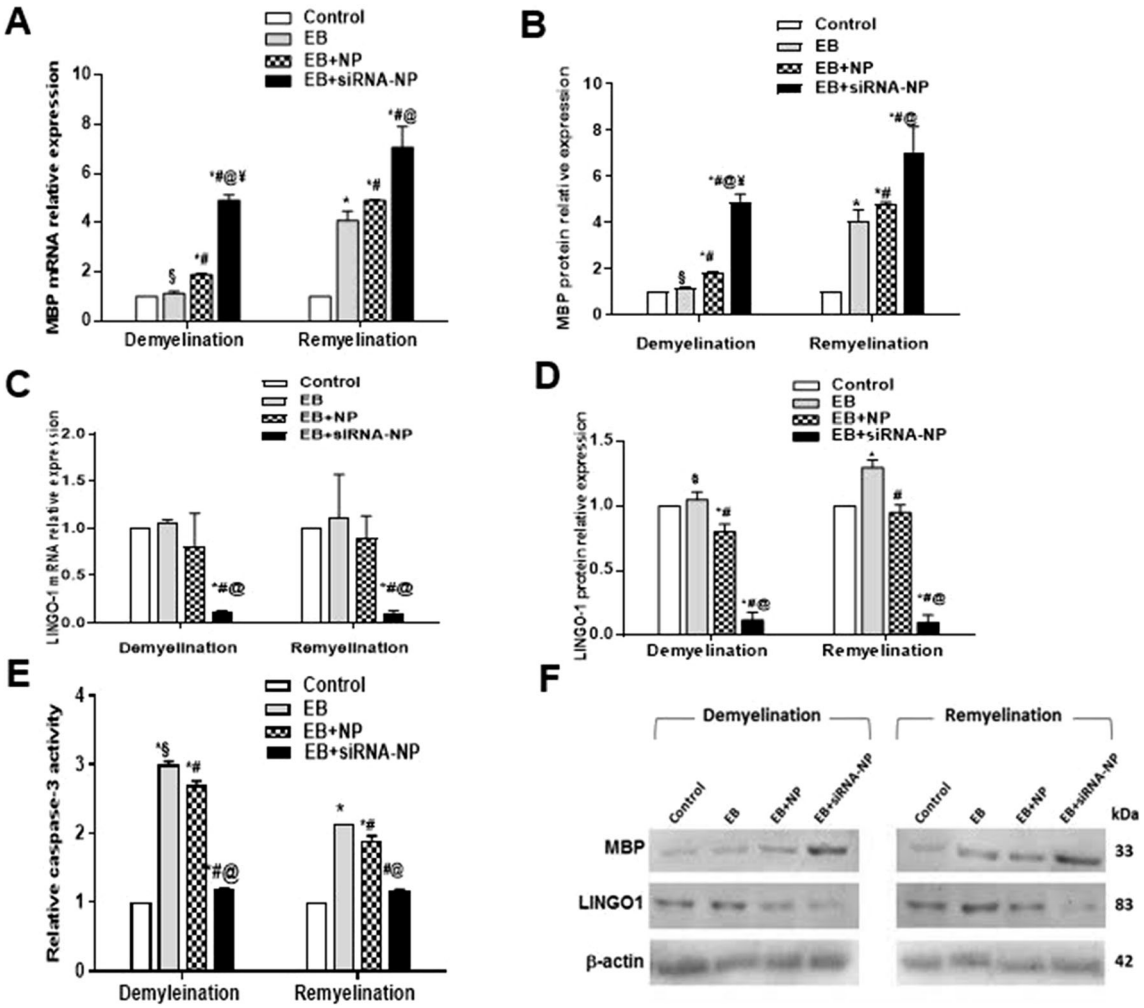

Fig. 2 Influence of LINGO-1–directed siRNA-loaded nanoparticle treatment on (**a**) MBP mRNA expression, (**b**) MBP protein expression, (**c**) LINGO-1 mRNA expression, (**d**) LINGO-1 protein expression, (**e**) caspase-3 activity, (**f**) Western blot analysis of MBP and LINGO-1 proteins in the pontine tissue homogenate after ethidium bromide injection in de- and remyelination groups. Results are shown as mean ± SD from $n = 10$ rats/group. Significant post hoc effects are indicated by asterisks $*p < 0.05$ versus corresponding control group, $\#p < 0.05$ versus corresponding ethidium bromide group, $@p < 0.05$ versus corresponding EB + NP groups, $\S p < 0.05$ between ethidium bromide groups, $¥p < 0.05$ between the EB + siRNA-NP groups

not mRNA, expression which might be a consequence to the possible improvement of neural pathology after chitosan nanoparticle administration.

LINGO-1–directed siRNA-loaded nanoparticles improved tissue remyelination

Histopathological analysis revealed that compared to control brains (Fig. 3a, b), EB injection led to active demyelination as evidenced by loosely textured neuropil meshwork (status spongiosus), with pyknotic fragmented nuclei. Brisk inflammatory cellular infiltrate is rich in macrophages with well-defined cell boundaries and foamy cytoplasm (Fig. 3c, d). After 21 days of EB injection, there were less areas of demyelination and inflammatory infiltrate (Fig. 3e, f). Histological examination of pontine tissue of rats in the treated remyelination group showed more compact myelin sheath within the demyelinated lesion, with a moderately intense chronic non-specific inflammatory cellular infiltrate rich in lymphocytes. The sub-ependymal area showed brisk angiogenesis which was evident by a newly formed blood vessel with plump endothelial lining and a surrounding cuff of inflammatory cells indicating reparative changes. These findings are suggestive of ongoing remyelination of the lost myelin sheaths (Fig. 3g, h).

Light micrograph images of pontine sections stained with LFB in control rats appeared intact with long oriented bundles of white matter denoting no destruction of the myelin sheath (Fig. 4a, b). Seven days after EB injection (Fig. 4c, d) showed different levels of staining in the demyelinated area. The spongy appearance is typical of vacuolar myelinolysis. Degeneration of myelin sheath was demonstrated which

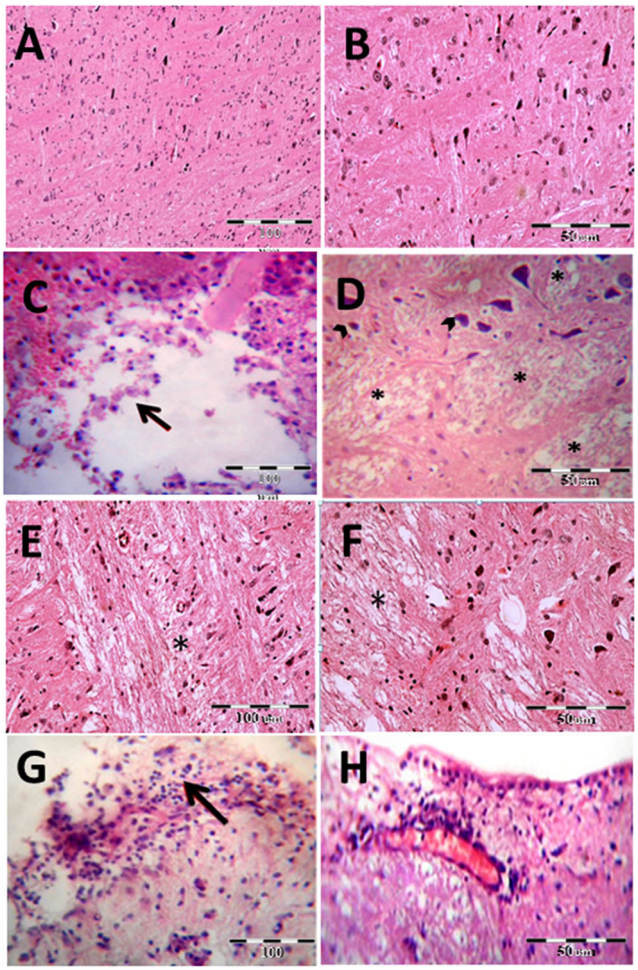

Fig. 3 Light micrograph of pontine tissue sections stained with H&E. Control rats, **a** and **b**, showed normal pattern of neuropil myelination and density. **c**, **d** after 7 days of EB injection showed active areas of demyelination (*) with loose neuropil and inflammatory cellular infiltrate rich in macrophages with foamy cytoplasm and enlarged white matter field. Pyknotic fragmented nuclei were observed ((⍟)). **e**, **f** After 21 days of EB injection showed less areas of demyelination and inflammatory infiltrate. **g**, **h** sections of pontine tissue in remyelination group treated with LINGO-1–directed siRNA chitosan nanoparticles showed more compact myelin sheath and moderately intense chronic non-specific inflammatory infiltrate rich in lymphocytes (arrow). Angiosis was observed in the subependymal area. **a**, **c**, **e**, **g** scale bars denote 100 μm and **b**, **d**, **f**, **h** scale bars denote 50 μm

indicate neurotoxicity. The demyelination sites were predominantly occupied by the demyelinated axons with debris of myelin sheaths. Administration of siRNA-loaded nanoparticles from day 1 partially protects the axons from demyelination as observed in images (Fig. 4e, f), with intact myelinated nerve fibres separated by a widened interfasicular spaces.

After 21 days of EB injection, the lesions showed less areas of demyelination (Fig. 4g, h), but still, there is interrupted pattern of white matter bundles (Fig. 4i, j). Sections of pontine tissue in remyelination group treated with LINGO-1–directed siRNA nanoparticles revealed better remyelination and more compact myelin sheath when compared with remyelination group treated with chitosan nanoparticles only (Fig. 4k, l).

Discussion

Current advances in MS therapy aim to improve remyelination and enhance signalling pathways required for new myelin formation. LINGO-1 inhibition is one of the most important recently used strategies to enhance remyelination in different animal models of CNS demyelination. Remyelination depends on the well-characterised population of OPCs, which differentiate into mature oligodendrocytes, which in turn, repair demyelinated lesions [12].

Stereotaxic injection of a gliotoxic compound as EB has been successfully used to trigger demyelination. The EB model features an extended demyelination lesion with clear temporal separation between de- and remyelination processes, in contrast to experimental autoimmune encephalomyelitis (EAE) and viral models of demyelination which induce small demyelination lesions with simultaneous demyelination and remyelination [16, 38].

Impairment in motor power and loss of stability was extremely manifested after EB injection in this study. The beam balance measures both muscle strength and coordination. Rats showed compromised test scores after EB injection since performance on the beam balance requires intense interhemispheric connections that are markedly damaged after EB injection [19]. Impairment of locomotor activity and coordination as evidenced by the foot fault and rotarod tests was also observed. Such impairment is attributed to demyelination of the nerve fibres as a results of apoptotic death of oligodendrocytes after EB injection as well as persistent inflammation [4].

LINGO-1–directed siRNA nanoparticle treatment improved the rat motor performance, more so in the delayed treatment group compared to early treatment. This suggests that spontaneous myelin repair correlates with partial restoration of neurological function following EB-induced toxic demyelination. However, neither early nor delayed treatment managed to completely normalise motor performance which is on line with previous studies showing slow recovery after EB injection due to slow removal of myelin debris [34].

Therefore, an association between remyelination and partial restoration of neurological function after toxic demyelination was noticed, such functional improvement occurred despite toxic demyelination. Myelin repair is believed to contribute to the recovery of some neurological function after acute attacks of inflammatory demyelination in MS [31].

Motor performance was significantly improved after LINGO-1–directed siRNA-loaded nanoparticle treatment particularly when started late from day 7–21. Such improvement may be correlated with features of myelin repair and angiogenesis in the studied pontine tissues. The use of LINGO-1

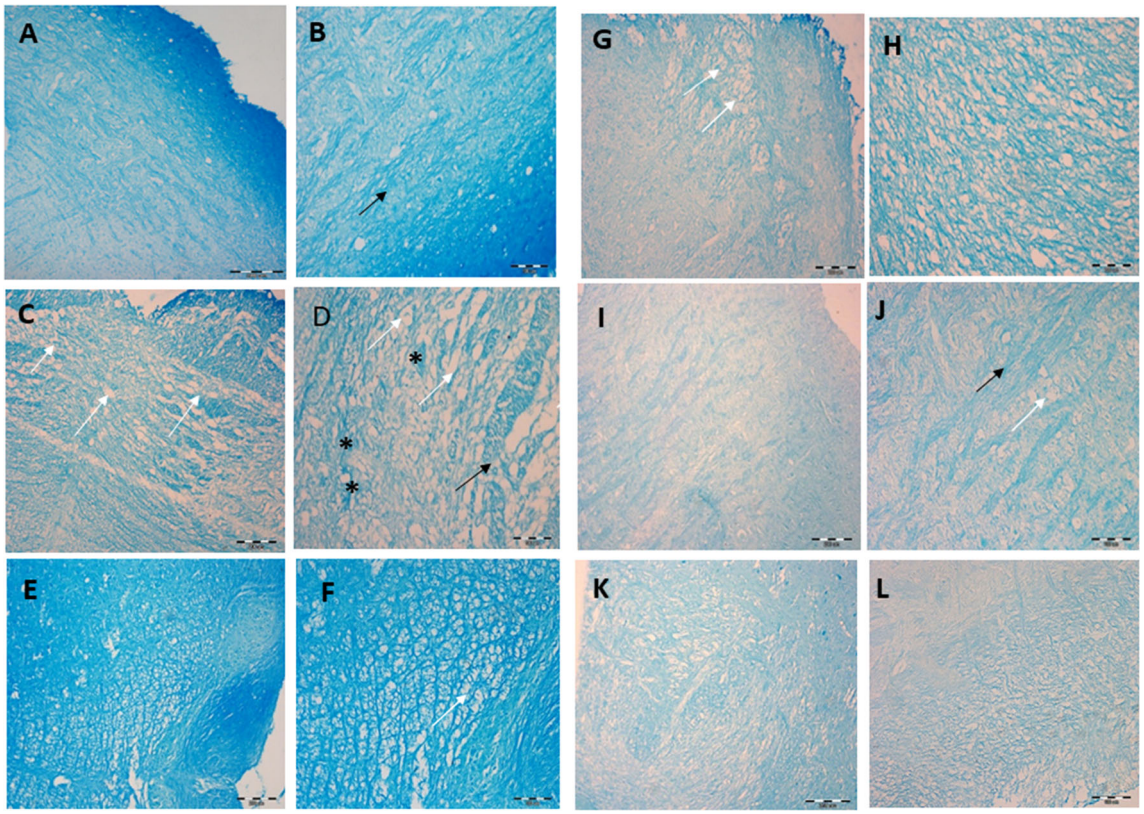

Fig. 4 Light micrograph images of pontine sections stained with LFB in control rats (Fig. 4**a**, **b**) appeared intact with long oriented bundles of white matter (arrows) denoting no destruction of the myelin sheath. Seven days after EB injection (**c**, **d**) showed different levels of staining in the demyelinated area (white arrows). The spongy appearance is typical of vacuolar myelinolysis (white arrows). Degeneration of myelin sheath was demonstrated which indicate neurotoxicity. The demyelination sites were predominantly occupied by the demyelinated axons with debris of myelin sheaths (*). Administration of siRNA-loaded nanoparticles from day 1 partially protects the axons from demyelination as observed in images (**e**, **f**). Intact myelinated nerve fibres are separated by a widened interfasicular spaces. After 21 days of EB injection, the lesions showed less areas of demyelination (**g**, **h**), but still, there is interrupted pattern of white matter bundles. **i**, **j** sections of pontine tissue in remyelination group treated with LINGO-1–directed siRNA nanoparticles revealed better remyelination and more compact myelin sheath when compared with remyelination group treated with chitosan nanoparticles only (**k**, **l**). Black arrows indicate splitting of the fibres and degree of compactness of the white matter fibre bundles. Scale bar denotes 200 μm in **a**, **c**, **e**, **g**, **i**, **k** and 100 μm in **b**, **d**, **f**, **h**, **j**, **l**

antagonist was found by several researchers to promote functional recovery and nerve regeneration after demyelination [22, 37]. Such effects could be attributed to increased neuronal and oligodendrocyte cell survival after LINGO-1 downregulation.

LINGO-1 downregulation is able to enhance remyelination and plasticity in the injured neural cells, by promoting sprouting from intact collateral axons [22, 30]. Previous findings obtained from in vitro and animal studies suggest that LINGO-1 suppression may be beneficial in neurodegenerative disorders such as Parkinson's disease and MS [2, 15]. Anti-LINGO-1 antibody (BIIB033) has been investigated as a potential remyelinating and axonal protective agent in people with MS [8, 35]. LINGO-1 level did not show any change after EB injection in early demyelination or late remyelination groups; EB as a gliotoxic is able to induce damage to various cell types as endothelial, astrocytes, oligodendrocytes and their precursors [5, 10]. LINGO-1 is known to be expressed earlier in the pre-myelinating oligodendrocytes rather than mature oligodendrocyte [33].

The siRNA offers a great potential as a highly specific, safe and efficient technique for silencing of a target gene [14]. Regarding the delivery systems of these RNA molecules, there are currently two major kinds of in vivo delivery systems: non-viral or viral [27]. The advantages of non-viral vectors include lower toxicity, lower immune-responsiveness and easy handling properties [28]. Chitosan is a natural, non-toxic polysaccharide [13]. In addition, the intranasal (IN) route of chitosan administration represents a non-invasive method to bypass the BBB and directly deliver drugs to the CNS along extracellular pathways [3].

Myelin basic protein is a component of the myelin sheath. For successful repair of myelin sheath, a strong and timely production of myelin proteins is needed [25]. Both immature and mature oligodendrocytes express MBP and, in this way, its expression can be regarded as an indicator for activity or presence of these cells [18]. The current study showed that on day 7 after EB injection, the pontine level of MBP expression was nearly the same as controls, then significantly increased

on day 21after EB injection compared with its level on day 7. Goudarzvand et al. reported that the expression of MBP in the lesioned hippocampus was significantly reduced 2 days after lesion then returned to control level on day 7, and exceeded the level of the control group on day 28 after EB injection [18]. This can be explained by oligodendrocyte damage and death on day 2, while the elevation of MBP expression to control level is attributed to the migration of precursor cells to the demyelination site and then their differentiation to oligodendrocytes on day 7 [38]. The age of myelinating cells affects the MBP level; therefore, the presence of younger cells in the remyelinated area than in the healthy control white matter would lead to a higher MBP expression [18]. Treatment with LINGO-1–directed siRNA nanoparticles, in the current study, resulted in significant elevation of MBP mRNA and protein expression in the remyelination group compared to the control group and remyelination untreated group. This can be explained by inhibition of LINGO-1 protein expression mediated by siRNA. However, MBP mRNA and protein was significantly higher in with late treatment (7–21 day) compared with the early treatment (1–7 days). This result is in agreement with Bourikas et al. [6], who found that LINGO-1 expression in oligodendroglial cells during differentiation resulted in restriction of extension and the transcription of MBP mRNA. Also, it was found that inhibition of synthesis of LINGO-1 protein by RNA interference leads to differentiation and enhancement of myelination competence in vitro [37]. Another interesting finding in the present work was the increase in MBP mRNA and protein expression after chitosan nanoparticle administration where such effect was more pronounced when the nanoparticles were coupled with LINGO-1 siRNA. Such finding refers to chitosan itself as a part of the neural effect of LINGO-1 siRNA-loaded nanoparticles. In this context, previous studies reported the antioxidant and anti-inflammatory potentials of chitinous materials [22]. Additionally, chitosan nanoparticles were claimed for their neuroprotective effect in several neurodegenerative diseases such as Alzheimer's disease [20, 29, 36].

Multiple sclerosis is mediated in part by an apoptotic mechanism which is characterised by caspase enzyme activation [18]. Therefore, relative caspase-3 activity in the pontine tissue was measured using colorimetric reaction to detect the degree of neural apoptosis. Results showed that following the local injection of EB, the ratio of activated caspase-3 was tripled on day 7 in demyelination group when compared to control group. Also, the remyelination group showed higher caspase-3 activity compared to the control group. EB injection and the associated demyelination of oligodendrocytes and apoptotic cell death were negatively correlated with pontine MBP mRNA and protein expression. These apoptotic changes may be due to activation of T cells and macrophages which produce inflammatory cytokines and mediators such as tumour necrosis factor (TNF)-a, interferon (IFN)-c and reactive oxygen/nitrogen species [18]. Degenerative changes, induced by EB injection into rat brain, are reported in oligodendrocytes within 72 h with subsequent death and demyelination.

Administration of LINGO-1–directed siRNA nanoparticles resulted in significant reduction in the level of caspase-3 activity in treated demyelination and remyelination groups when compared with untreated groups. This result can be supported by Wu et al. [37] who found that injection of lentiviral vectors encoding LINGO-1 shRNA promoted the neural survival and decreased apoptotic cells adjacent to the injured site in a model of spinal cord injury [37]. Inhibition of apoptosis can explain preservation of motor performance in treated demyelination group and the improvement that occurred in treated remyelination group. The current study further reports the potential anti-apoptotic effect of chitosan nanoparticles where this effect was intensified when the nanoparticles coupled with LINGO-1 siRNA further emphasising its potential neuroprotective effect and enhancing the effect of the coupled siRNA. Concerning apoptosis, chitosan was reported to protect against neural apoptosis [31, 38] which adds to the advantages of coupling chitosan nanoparticles with LINGO-1 siRNA as a possible therapy for MS.

Conclusion

The present study concluded that LINGO-1–directed siRNA-loaded chitosan nanoparticles can improve neurological, neurochemical disturbance and enhance remyelination in EB-induced demyelination rat model. Intranasal way of administration of LINGO-1–directed siRNA nanoparticles appears to be an effective tool for drug delivery. It is worth mentioning that the current study revealed that the treatment regimen may exert great effect on the outcome. Improvement of biochemical parameters, motor performance and histopathological finding was significantly better when the treatment strategy is applied for 2 weeks in remyelination phase when compared to its usage as neuroprotective agent in demyelination phase.

Acknowledgements The authors are grateful to Dr. Teshreen M. Zeitoun, Ass. Prof in the Department of Medical Histology and Cell Biology-Alexandria Faculty of Medicine for her great support in Luxol fast blue staining and interpretation; and to Dr. Bassma El-Saba, Professor of Pathology-Alexandria Faculty of Medicine for her assistance in the histopathology analysis.

Compliance with ethical standards

Ethical approval All applicable international, national, and/or institutional guidelines for the care and use of animals were followed. Additionally, all procedures performed involving animals were in accordance with the ethical standards of Alexandria University, Egypt.

Conflict of interest The authors declare that they have no conflict of interest.

Publisher's note Springer Nature remains neutral with regard to jurisdictional claims in published maps and institutional affiliations.

References

1. Aartsma-Rus A, van Putten M (2014) Assessing functional performance in the mdx mouse model. J Vis Exp. https://doi.org/10.3791/51303
2. Agundez JA, Jimenez-Jimenez FJ, Alonso-Navarro H, Garcia-Martin E (2015) The potential of LINGO-1 as a therapeutic target for essential tremor. Expert Opin Ther Targets 19:1139–1148. https://doi.org/10.1517/14728222.2015.1028360
3. Al-Ghananeem AM, Saeed H, Florence R, Yokel RA, Malkawi AH (2010) Intranasal drug delivery of didanosine-loaded chitosan nanoparticles for brain targeting; an attractive route against infections caused by AIDS viruses. J Drug Target 18:381–388. https://doi.org/10.3109/10611860903483396
4. Beckmann DV, Carvalho FB, Mazzanti CM, Dos Santos RP, Andrades AO, Aiello G, Rippilinger A, Graca DL, Abdalla FH, Oliveira LS, Gutierres JM, Schetinger MR, Mazzanti A (2014) Neuroprotective role of quercetin in locomotor activities and cholinergic neurotransmission in rats experimentally demyelinated with ethidium bromide. Life Sci 103:79–87. https://doi.org/10.1016/j.lfs.2014.03.033
5. Bondan EF, Martins Mde F, Bernardi MM (2015) Propentofylline reverses delayed remyelination in streptozotocin-induced diabetic rats. Arch Endocrinol Metab 59:47–53. https://doi.org/10.1590/2359-3997000000009
6. Bourikas D, Mir A, Walmsley AR (2010) LINGO-1-mediated inhibition of oligodendrocyte differentiation does not require the leucine-rich repeats and is reversed by p75(NTR) antagonists. Mol Cell Neurosci 45:363–369. https://doi.org/10.1016/j.mcn.2010.07.009
7. Boyd A, Zhang H, Williams A (2013) Insufficient OPC migration into demyelinated lesions is a cause of poor remyelination in MS and mouse models. Acta Neuropathol 125:841–859. https://doi.org/10.1007/s00401-013-1112-y
8. Cadavid D, Balcer L, Galetta S, Aktas O, Ziemssen T, Vanopdenbosch L, Butzkueven H, Ziemssen F, Massacesi L, Chai Y, Xu L, Freeman S (2015) Efficacy analysis of the anti-LINGO-1 monoclonal antibody BIIB033 in acute optic neuritis: the RENEW trial Neurology 84:Poster p7.202
9. Cao J, Wang J, Dwyer JB, Gautier NM, Wang S, Leslie FM, Li MD (2013) Gestational nicotine exposure modifies myelin gene expression in the brains of adolescent rats with sex differences. Transl Psychiatry 3:e247. https://doi.org/10.1038/tp.2013.21
10. Caprariello AV, Mangla S, Miller RH, Selkirk SM (2012) Apoptosis of oligodendrocytes in the central nervous system results in rapid focal demyelination. Ann Neurol 72:395–405. https://doi.org/10.1002/ana.23606
11. Casciola-Rosen L, Nicholson DW, Chong T, Rowan KR, Thornberry NA, Miller DK, Rosen A (1996) Apopain/CPP32 cleaves proteins that are essential for cellular repair: a fundamental principle of apoptotic death. J Exp Med 183:1957–1964
12. Chang A, Staugaitis SM, Dutta R, Batt CE, Easley KE, Chomyk AM, Yong VW, Fox RJ, Kidd GJ, Trapp BD (2012) Cortical remyelination: a new target for repair therapies in multiple sclerosis. Ann Neurol 72:918–926. https://doi.org/10.1002/ana.23693
13. Corbet C, Ragelle H, Pourcelle V, Vanvarenberg K, Marchand-Brynaert J, Preat V, Feron O (2016) Delivery of siRNA targeting tumor metabolism using non-covalent PEGylated chitosan nanoparticles: identification of an optimal combination of ligand structure, linker and grafting method. J Control Release 223:53–63. https://doi.org/10.1016/j.jconrel.2015.12.020
14. Davis ME, Zuckerman JE, Choi CHJ, Seligson D, Tolcher A, Alabi CA, Yen Y, Heidel JD, Ribas A (2010) Evidence of RNAi in humans from systemically administered siRNA via targeted nanoparticles. Nature 464:1067–1070. https://doi.org/10.1038/nature08956
15. Deiss A, Brecht I, Haarmann A, Buttmann M (2013) Treating multiple sclerosis with monoclonal antibodies: a 2013 update. Expert Rev Neurother 13:313–335. https://doi.org/10.1586/ern.13.17
16. Dubois-Dalcq M, Ffrench-Constant C, Franklin RJ (2005) Enhancing central nervous system remyelination in multiple sclerosis. Neuron 48:9–12. https://doi.org/10.1016/j.neuron.2005.09.004
17. El-Tallawy HN, Farghaly WMA, Badry R, Metwally NA, Shehata GA, Rageh TA, El Hamed MA, Kandil MR (2016) Prevalence of multiple sclerosis in Al Quseir city, Red Sea Governorate, Egypt. Neuropsychiatr Dis Treat 12:155–158. https://doi.org/10.2147/NDT.S87348
18. Goudarzvand M, Javan M, Mirnajafi-Zadeh J, Mozafari S, Tiraihi T (2010) Vitamins E and D3 attenuate demyelination and potentiate remyelination processes of hippocampal formation of rats following local injection of ethidium bromide. Cell Mol Neurobiol 30:289–299. https://doi.org/10.1007/s10571-009-9451-x
19. Hagemeyer N, Boretius S, Ott C, Von Streitberg A, Welpinghus H, Sperling S, Frahm J, Simons M, Ghezzi P, Ehrenreich H (2012) Erythropoietin attenuates neurological and histological consequences of toxic demyelination in mice. Mol Med 18:628–635. https://doi.org/10.2119/molmed.2011.00457
20. Hao C, Wang W, Wang S, Zhang L, Guo Y (2017) An overview of the protective effects of chitosan and acetylated chitosan oligosaccharides against neuronal disorders. Mar Drugs 15. https://doi.org/10.3390/md15040089
21. Hernandez TD, Schallert T (1988) Seizures and recovery from experimental brain damage. Exp Neurol 102:318–324
22. Ji B, Li M, Wu WT, Yick LW, Lee X, Shao Z, Wang J, So KF, McCoy JM, Pepinsky RB, Mi S, Relton JK (2006) LINGO-1 antagonist promotes functional recovery and axonal sprouting after spinal cord injury. Mol Cell Neurosci 33:311–320. https://doi.org/10.1016/j.mcn.2006.08.003
23. Kim ID, Shin JH, Kim SW, Choi S, Ahn J, Han PL, Park JS, Lee JK (2012) Intranasal delivery of HMGB1 siRNA confers target gene knockdown and robust neuroprotection in the postischemic brain. Mol Ther 20:829–839. https://doi.org/10.1038/mt.2011.291
24. Mi S, Lee X, Shao Z, Thill G, Ji B, Relton J, Levesque M, Allaire N, Perrin S, Sands B, Crowell T, Cate RL, McCoy JM, Pepinsky RB (2004) LINGO-1 is a component of the Nogo-66 receptor/p75 signaling complex. Nat Neurosci 7:221–228. https://doi.org/10.1038/nn1188
25. Michel K, Zhao T, Karl M, Lewis K, Fyffe-Maricich SL (2015) Translational control of myelin basic protein expression by ERK2 MAP kinase regulates timely remyelination in the adult brain. J Neurosci 35:7850–7865. https://doi.org/10.1523/jneurosci.4380-14.2015
26. Munzel EJ, Williams A (2013) Promoting remyelination in multiple sclerosis-recent advances. Drugs 73:2017–2029. https://doi.org/10.1007/s40265-013-0146-8
27. Nayerossadat N, Maedeh T, Ali PA (2012) Viral and nonviral delivery systems for gene delivery. Adv Biomed Res 1:27. https://doi.org/10.4103/2277-9175.98152
28. Nishikawa M, Yamauchi M, Morimoto K, Ishida E, Takakura Y, Hashida M (2000) Hepatocyte-targeted in vivo gene expression by intravenous injection of plasmid DNA complexed with synthetic multi-functional gene delivery system. Gene Ther 7:548–555. https://doi.org/10.1038/sj.gt.3301140
29. Pangestuti R, Kim SK (2010) Neuroprotective properties of chitosan and its derivatives. Mar Drugs 8:2117–2128. https://doi.org/10.3390/md8072117

30. Pepinsky RB, Shao Z, Ji B, Wang Q, Meng G, Walus L, Lee X, Hu Y, Graff C, Garber E, Meier W, Mi S (2011) Exposure levels of anti-LINGO-1 Li81 antibody in the central nervous system and dose-efficacy relationships in rat spinal cord remyelination models after systemic administration. J Pharmacol Exp Ther 339:519–529. https://doi.org/10.1124/jpet.111.183483
31. Podbielska M, Banik NL, Kurowska E, Hogan EL (2013) Myelin recovery in multiple sclerosis: the challenge of remyelination. Brain Sci 3:1282–1324. https://doi.org/10.3390/brainsci3031282
32. Ragelle H, Riva R, Vandermeulen G, Naeye B, Pourcelle V, Le Duff CS, D'Haese C, Nysten B, Braeckmans K, De Smedt SC, Jerome C, Preat V (2014) Chitosan nanoparticles for siRNA delivery: optimizing formulation to increase stability and efficiency. J Control Release 176:54–63. https://doi.org/10.1016/j.jconrel.2013.12.026
33. Satoh J, Tabunoki H, Yamamura T, Arima K, Konno H (2007) TROY and LINGO-1 expression in astrocytes and macrophages/microglia in multiple sclerosis lesions. Neuropathol Appl Neurobiol 33:99–107. https://doi.org/10.1111/j.1365-2990.2006.00787.x
34. Shields SA, Gilson JM, Blakemore WF, Franklin RJ (1999) Remyelination occurs as extensively but more slowly in old rats compared to young rats following gliotoxin-induced CNS demyelination. Glia 28:77–83
35. Tran JQ, Rana J, Barkhof F, Melamed I, Gevorkyan H, Wattjes MP, de Jong R, Brosofsky K, Ray S, Xu L, Zhao J, Parr E, Cadavid D (2014) Randomized phase I trials of the safety/tolerability of anti-LINGO-1 monoclonal antibody BIIB033. Neurol Neuroimmunol Neuroinflamm 1:e18. https://doi.org/10.1212/nxi.0000000000000018
36. Wei P, Ma P, Xu QS, Bai QH, Gu JG, Xi H, Du YG, Yu C (2012) Chitosan oligosaccharides suppress production of nitric oxide in lipopolysaccharide-induced N9 murine microglial cells in vitro. Glycoconj J 29:285–295. https://doi.org/10.1007/s10719-012-9392-3
37. Wu HF, Cen JS, Zhong Q, Chen L, Wang J, Deng DY, Wan Y (2013) The promotion of functional recovery and nerve regeneration after spinal cord injury by lentiviral vectors encoding Lingo-1 shRNA delivered by Pluronic F-127. Biomaterials 34:1686–1700. https://doi.org/10.1016/j.biomaterials.2012.11.013
38. Zhao C, Fancy SP, Kotter MR, Li WW, Franklin RJ (2005) Mechanisms of CNS remyelination–the key to therapeutic advances. J Neurol Sci 233:87–91. https://doi.org/10.1016/j.jns.2005.03.008